

Swift/XRT monitoring of five orbital cycles of LSI+61° 303

P. Esposito^{1,2}, P. A. Caraveo², A. Pellizzoni², A. De Luca², N. Gehrels³, and M. A. Marelli²

¹ Università degli Studi di Pavia, Dipartimento di Fisica Nucleare e Teorica and INFN-Pavia, via Bassi 6, 27100 Pavia, Italy
e-mail: paoloesp@iasf-milano.inaf.it

² INAF – Istituto di Astrofisica Spaziale e Fisica Cosmica Milano, via Bassini 15, 20133 Milano, Italy

³ NASA/Goddard Space Flight Center, Greenbelt, Maryland 20771, USA

Received 23 July 2007 / Accepted 16 August 2007

ABSTRACT

Context. LSI+61° 303 is one of the most interesting high-mass X-ray binaries owing to its spatially resolved radio emission and its TeV emission, generally attributed to non-thermal particles in an accretion-powered relativistic jet or in the termination shock of the relativistic wind of a young pulsar. Also, the nature of the compact object is still debated. Only LS 5039 and PSR B1259–63 (which hosts a non-accreting millisecond pulsar) have similar characteristics.

Aims. We study the X-ray emission from LSI+61° 303 covering both short-term and orbital variability. We also investigate the source spectral properties in the soft X-ray (0.3–10 keV) energy range.

Methods. Twenty-five snapshot observations of LSI+61° 303 were collected in 2006 with the XRT instrument on-board the *Swift* satellite over a period of four months, corresponding to about five orbital cycles. Since individual data sets have too few counts for a meaningful spectral analysis, we extracted a cumulative spectrum.

Results. The count rate folded at the orbital phase shows a clear modulation pattern at the 26.5 days period and suggests that the X-ray peak occurs around phase 0.65. Moreover, the X-ray emission appears to be variable on a timescale of ~1 ks. The cumulative spectrum is well described by an absorbed power-law model, with hydrogen column density $N_{\text{H}} = (5.7 \pm 0.3) \times 10^{21} \text{ cm}^{-2}$ and photon index $\Gamma = 1.78 \pm 0.05$. No accretion disk signatures, such as an iron line, are found in the spectrum.

Key words. X-rays: individual: LSI+61° 303 – X-rays: binaries

1. Introduction

LSI+61° 303 is a peculiar binary system characterized by variable radio emission, long known to be modulated with a 26.4960 ± 0.0028 days orbital period (Gregory & Taylor 1978; Gregory 2002). The eccentricity of the orbit is 0.72 ± 0.15 , and the periastron passage occurs at phase $\phi = 0.23 \pm 0.02$ (Casares et al. 2005). The phase of the radio maximum shifts between $0.45 \leq \phi \leq 0.9$ with a 1667 ± 8 days period (Gregory 2002), pointing to a second modulation. HI observations of the radio source give a distance of 2.0 ± 0.2 kpc (Frail & Hjellming 1991), implying an X-ray luminosity of $\sim 10^{33} \text{ erg s}^{-1}$. Optical studies have established the primary star to be a Be surrounded by a small and inhomogeneous disk whose optical and H α emission is also modulated (Hutchings & Crampton 1981; Mendelson & Mazeh 1989; Paredes et al. 1994; Zamanov et al. 1999).

LSI+61° 303 has been attracting a lot of attention (and observing time) owing to its putative link with the gamma-ray source 2CG 135+01, discovered by *COS-B* (Hermsen et al. 1977; Swanenburg et al. 1981; Bignami & Hermsen 1983) 30 years ago and later confirmed by *CGRO/EGRET*, as 3EG J0241+6103 (Hartman et al. 1999), with observations spanning the period 1991–2000. In spite of relentless efforts (Tavani et al. 1996; Kniffen et al. 1997), no conclusive evidence for the orbital modulation was found in the gamma-ray data, thus hampering the source identification. Recently the orbital modulation was seen by the *MAGIC* Cherenkov air-showers telescope in ultra high energy gamma rays (above 400 GeV), clinching the case for the identification of LSI+61° 303 as a gamma-ray emitter (Albert et al. 2006). This was also confirmed in the hard

X-ray energies (up to 100 keV) by *INTEGRAL* observation of variable emission, peaking at phase ~ 0.55 of the orbital modulation (Chernyakova et al. 2006; Hermsen & Kuiper 2007).

Although in soft X-rays there were no doubts from the start about the source identification (Bignami et al. 1981), the X-ray observations, aimed at studying the orbital modulation, proceeded in parallel with the gamma-ray ones, using all the X-ray instruments active over the past 30 years: *Einstein* (Bignami et al. 1981), *ROSAT* (Goldoni & Mereghetti 1995; Taylor et al. 1996), *ASCA* (Leahy et al. 1997), *RossixTE* (Paredes et al. 1997; Harrison et al. 2000; Greiner & Rau 2001; Leahy 2001; Grundstrom et al. 2007), *INTEGRAL* (Chernyakova et al. 2006; Hermsen & Kuiper 2007), *BeppoSAX*, *XMM-Newton* (Sidoli et al. 2006), and *Chandra* (Paredes et al. 2007).

Today, the behavior of LSI+61° 303 continues to defy easy characterization. Its X-ray emission appears to be variable over both long and short time scales (e.g., Sidoli et al. 2006), hampering the detection of an unambiguous modulation pattern when only sparse observations are available. Here we report the monitoring of the source soft X-ray flux over 5 adjacent orbital cycles, using the XRT telescope onboard the NASA/UK/ASI *Swift* mission (Gehrels et al. 2004).

2. Observations and analysis

Twenty-five *Swift* observations of LSI+61° 303 have been performed with the XRT instrument in photon counting (PC) mode (Burrows et al. 2005). The XRT uses a CCD detector sensitive to photons with energies between 0.2 and 10 keV. Table 1 reports the log of the *Swift*/XRT observations used for this work.

Table 1. Observation log.

Sequence	Start time (UT) (yyyy-mm-dd hh:mm:ss)	End time (UT) (yyyy-mm-dd hh:mm:ss)	Phase ^a	Net exposure ^b (s)	Count rate ^c (counts s ⁻¹)
00036093001	2006-09-02 08:09:31	2006-09-02 11:46:56	0.591–0.597	4665	0.271 ± 0.008
00036093002	2006-09-05 21:39:40	2006-09-05 23:22:56	0.726–0.728	749	0.22 ± 0.02
00036093003	2006-09-11 00:57:04	2006-09-11 23:30:56	0.920–0.955	4657	0.120 ± 0.005
00036093004	2006-09-13 09:40:21	2006-09-13 22:36:57	0.009–0.029	3598	0.187 ± 0.007
00036093005	2006-09-15 07:56:34	2006-09-15 13:11:57	0.082–0.090	3783	0.223 ± 0.008
00036093006	2006-09-17 06:33:09	2006-09-17 09:54:58	0.155–0.160	3559	0.091 ± 0.005
00036093007	2006-09-19 09:53:05	2006-09-19 14:57:57	0.236–0.244	2053	0.117 ± 0.008
00036093008	2006-11-21 01:56:37	2006-11-21 08:22:56	0.601–0.611	3024	0.226 ± 0.009
00036093009	2006-11-22 03:28:09	2006-11-22 08:27:56	0.641–0.649	3965	0.219 ± 0.007
00036093010	2006-11-23 01:59:58	2006-11-23 07:01:56	0.676–0.684	3092	0.30 ± 0.01
00036093011	2006-11-24 03:47:00	2006-11-24 08:46:56	0.717–0.725	2976	0.30 ± 0.01
00036093012	2006-11-29 06:13:28	2006-11-29 08:02:56	0.909–0.912	1126	0.13 ± 0.01
00036093013	2006-11-30 06:18:01	2006-11-30 08:06:56	0.947–0.950	1900	0.22 ± 0.01
00036093014 ^d	2006-12-02 22:45:00	2006-12-02 22:45:57	0.049	58	0.24 ± 0.07
00036093016	2006-12-05 03:42:40	2006-12-05 13:23:58	0.132–0.147	1284	0.12 ± 0.01
00036093017	2006-12-07 03:47:46	2006-12-07 16:51:57	0.208–0.228	2455	0.065 ± 0.005
00036093018	2006-12-09 12:24:07	2006-12-09 16:59:57	0.297–0.304	2145	0.20 ± 0.01
00036093019	2006-12-11 00:51:08	2006-12-11 02:48:58	0.354–0.357	2097	0.076 ± 0.006
00036093020	2006-12-13 01:01:26	2006-12-13 09:07:57	0.430–0.442	1126	0.12 ± 0.01
00036093021	2006-12-14 01:09:47	2006-12-14 23:40:57	0.468–0.503	707	0.14 ± 0.01
00036093022	2006-12-16 01:21:46	2006-12-16 14:14:56	0.543–0.564	1633	0.19 ± 0.01
00036093023	2006-12-18 06:15:42	2006-12-18 17:36:58	0.627–0.644	2168	0.26 ± 0.01
00036093024	2006-12-20 19:19:35	2006-12-20 19:39:56	0.722–0.723	622	0.26 ± 0.02
00036093025	2006-12-22 00:12:58	2006-12-22 05:07:58	0.768–0.776	1393	0.13 ± 0.01
00036093026	2006-12-24 10:27:07	2006-12-24 15:21:56	0.860–0.867	2764	0.25 ± 0.01

^a Following Gregory (2002) we adopt as time of the zero phase $JD_0 = 2\,443\,366.775$, with the orbital period $P_{\text{orb}} = 26.4960 \pm 0.0028$ days. The mean error on the orbital phase is ± 0.002 . The phase of the super-orbital modulation of the orbital phase and amplitude of the radio outbursts (with a period of 1667 ± 8 days; Gregory 2002) spans from ~ 0.367 (observation 00036093001) to ~ 0.435 (observation 00036093026).

^b The exposure time is spread over several snapshots (single continuous pointings at the target) during each observation.

^c Hereafter all errors are at 1σ confidence level, unless otherwise specified.

^d This observation is listed for completeness, but will not be used for the analysis owing to its short integration time.

The data were processed with standard procedures using the FTOOLS¹ task `xrtpipeline` (version 0.10.6 under the Heasoft package 6.2.0). We selected events with grades 0–12 and limited the analysis between 0.3–10 keV, where the PC response matrices are well calibrated. We extracted the source events from a circular region with a radius of 20 pixels (1 pixel $\approx 2.37''$), whereas to account for the background we extracted events within an annular source-free region centered on LSI+61° 303 and with radii 55 and 75 pixels. Since the data show a maximum count rate < 0.3 counts s⁻¹, no pile-up correction was necessary.

Inspection of the XRT light curves relative to each observation shows evidence of moderate variability (up to a factor of ~ 4) on a timescale of ~ 1 ks (see Fig. 1), an effect already observed in X-rays with various instruments (e.g., Sidoli et al. 2006). However, the statistics are too poor to assess spectral variation as a function of the source count rate.

Individual data sets have too few counts for a meaningful spectral analysis. Therefore, we extracted a cumulative spectrum. This corresponds to a total exposure of 52.6 ks and contains about 10 000 net counts in the 0.3–10 keV range. The data were rebinned with a minimum of 20 counts per energy bin to allow χ^2 fitting. The ancillary response file was generated with `xrtmkarf`, and it accounts for different extraction regions, vignetting and point-spread function corrections. We used the latest available spectral redistribution matrix (`swxpc0to12_20010101v008.rmf`).

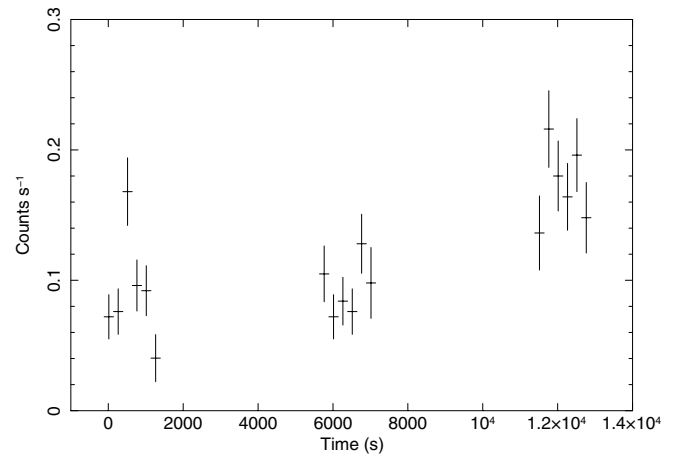


Fig. 1. *Swift*/XRT light curve of the first 14 ks of observation 00036093003 (see Table 1 for details). The bin size is 250 s and less than 0.001 counts s⁻¹ are expected from background events. The short-term X-ray variability of LSI+61° 303 is apparent.

The spectral fitting was performed using XSPEC² version 12.3, adopting an absorbed power-law model. We find the following best-fit ($\chi^2_{\text{red}} = 1.00$ for 359 degrees of freedom) parameters³: absorption $N_{\text{H}} = (5.7 \pm 0.3) \times 10^{21}$ cm⁻² and photon

² See <http://heasarc.gsfc.nasa.gov/docs/xanadu/xspec/>

³ Spectral errors are given at the 90% confidence level for a single interesting parameter.

¹ See <http://heasarc.gsfc.nasa.gov/docs/software/>

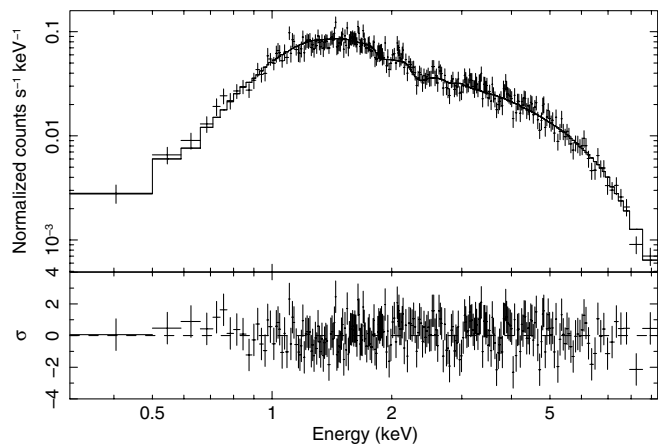


Fig. 2. *Swift*/XRT cumulative spectrum of LSI +61° 303 (see Sect. 2 for details). *Top*: data and best-fit power-law model. *Bottom*: residuals from the best-fit model in units of standard deviation.

index $\Gamma = 1.78 \pm 0.05$ (see Fig. 2). No evidence for emission or absorption lines was found by inspecting the residuals from the best-fit models (see Fig. 2). The addition of a blackbody component is not required. We used the resulting averaged flux (corrected for the absorption) of $\sim 2.2 \times 10^{-11} \text{ erg cm}^{-2} \text{ s}^{-1}$ to derive the conversion factor $1 \text{ count s}^{-1} \approx 1.1 \times 10^{-10} \text{ erg cm}^{-2} \text{ s}^{-1}$ in the 0.3–10 keV energy range. The mean count rate of each observation is reported in Table 1 and the values are plotted against the orbital radio phase in Fig. 3. First we provide an orbit-by-orbit view, then all the data are plotted together and finally they are averaged over a ~ 2.5 day bin corresponding to 1/10 of the radio orbital phase. The source luminosity ranges from $\sim 3.4 \times 10^{33} d_N^2 \text{ erg s}^{-1}$ to $\sim 1.6 \times 10^{34} d_N^2 \text{ erg s}^{-1}$, where we indicate with d_N the distance in units of N kpc.

3. Discussion

LSI +61° 303 is one of the most intriguing Be/X-ray binary systems because of its periodic radio and X-ray emission and of its strong gamma-ray emission. Two main models have been proposed to account for the peculiarities of LSI +61° 303 and of the similar binary LS 5039 (orbital period $P_{\text{orb}} = 3.9$ days; Paredes et al. 2000); see Mirabel (2006) for a recent review. The first model assumes that the systems are powered by accretion on either a neutron star or a black-hole, and that non-thermal particles are accelerated in relativistic jets. The second supposes that LSI +61° 303 and LS 5039 are similar to the rotation-powered system PSR B1259–63, composed by a millisecond radio pulsar orbiting around a Be star ($P_{\text{orb}} = 1237$ days and pulsar spin period of 47.7 ms; e.g., Kaspi et al. 1995). In this scenario, the non-thermal emission arises from the shock resulting from the interaction between the relativistic pulsar wind and the stellar wind originating from the companion star. The *Swift*/XRT monitoring of LSI +61° 303 over five orbital periods provides more elements to constrain the parameter space of the source.

We observed flux fluctuations up to a factor of ≈ 3 from the mean value at intra-hour scales. An example of this variability, already observed with various X-ray instruments (e.g., Sidoli et al. 2006), is given in Fig. 1. This kind of variability has also been observed in LS 5039, and it is generally interpreted as being due to variations or anisotropies in the stellar wind (Bosch-Ramon et al. 2005). The folding of the XRT count rates at the ~ 26.5 days period (Fig. 3) strongly suggests that this “flickering” is superimposed on an overall orbital modulation.

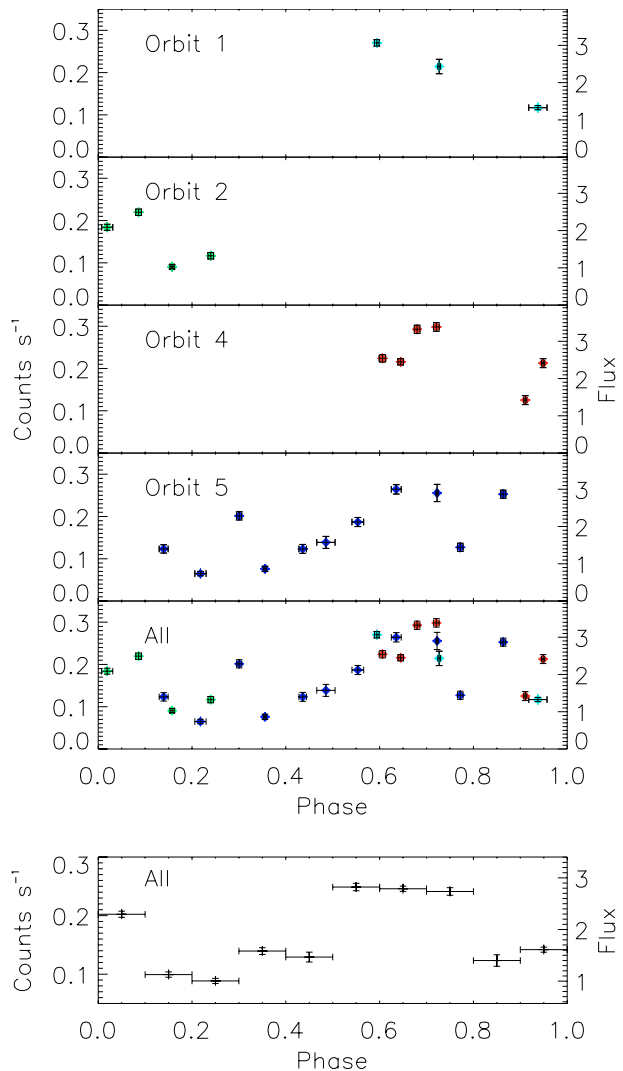


Fig. 3. *Swift*/XRT background-subtracted count rates folded as a function of the radio orbital phase (in the 0.3–10 keV energy range). The count rates have been converted to unabsorbed fluxes (in units of $10^{-11} \text{ erg cm}^{-2} \text{ s}^{-1}$) in the same energy range using the conversion factor given in Sect. 2. *Top*: on each panel, the data, averaged over a single observation, are plotted for different orbits (in the fifth panel all data are plotted simultaneously). *Bottom*: all data binned at 0.1 in phase are plotted simultaneously. See the online edition of the article for a color version of this figure.

We note that the erratic behavior of LSI +61° 303 should be carefully considered when assessing the orbital modulation pattern using observations of the source collected at different times.

Previous multi-wavelength campaigns undertaken with different instruments (Taylor et al. 1996; Harrison et al. 2000) indicate that the X-ray emission peak tends to precede the radio outburst by a few days. However, the exact phase of the X-ray maximum was difficult to estimate because of the poor sampling of the orbit of LSI +61° 303. Recently, folding more than 600 *INTEGRAL* pointings performed discontinuously with IBIS/ISGRI from March 2003 to July 2006 for a total exposure time of ~ 1.1 Ms, and *RossixTE*/ASM data from a similar time-span, Hermsen & Kuiper (2007) found a maximum at phase ~ 0.55 in the 1–100 keV band (in agreement with the results found by Paredes et al. (1997) and Grundstrom et al. (2007) based on *RossixTE*/ASM data only).

By binning the folded light curves in different ways, we estimate that a broad X-ray peak occurs around phase 0.65 (see Fig. 3), while the radio outburst is expected at phase $\approx 0.8\text{--}0.9$ (Gregory et al. 1999; Gregory 2002). The maximum X-ray flux is not detected at periastron ($\phi \approx 0.23$; Casares et al. 2005), where the accretion rate should reach its maximum value (Martí & Paredes 1995).

In the framework of the model invoking a shocked pulsar wind, X-ray flux peak and radio outburst could be in principle ascribed to the same particle population. Although significant inverse Compton losses should be at work (e.g., Dubus 2006; Sidoli et al. 2006), it is worth noting that the delay of ≈ 0.2 in phase ($\sim 5 \times 10^5$ s) between X-ray and radio peaks is compatible with synchrotron-dominated cooling rate of electrons with typical Lorentz factor of $\gamma \sim 10^5$ assuming a magnetic field of ~ 0.1 G in the post-shock distribution. Dubus (2006) predicts higher values (a few Gauss) for the magnetic field at a stand-off distance of $R_s \sim 10^{11}$ cm from the pulsar, but their theoretical estimate relies on as yet poorly constrained parameters such as pulsar spin-down energy and the ratio of magnetic to kinetic energy in the pulsar wind. In this context, the fact that both X-ray and radio peaks are not detected at periastron is not surprising, considering that shock strength could strongly depend on the anisotropic geometry of the pulsar wind, and not only on the separation between the two stars.

The data collected with the XRT detector can be described by a featureless power-law spectrum with photon index $\Gamma \sim 1.8$. Similar photon indices were also measured with other X-ray telescopes (e.g. Sidoli et al. 2006). This value fits reasonably well in a shock acceleration scenario where electrons and positrons cool slowly (Chevalier 2000), while spectra of high-mass accretion-powered X-ray binaries are generally harder ($\Gamma \approx 1$; e.g., White et al. 1983).

We remark that the spectral characteristics of LSI+61° 303 are similar to those of the Be/X-ray binary A 0538–66 (White & Carpenter 1978) in its present low-luminosity state. This system, situated in the Large Magellanic Cloud, was discovered as a source of X-ray flares showing a recurrence of 16.65 days, interpreted as the orbital period (Skinner 1980). Optical observations also unveiled a super-orbital modulation of ~ 421 days (Alcock et al. 2001). A 0538–66 contains a 69 ms X-ray pulsar (Skinner et al. 1982) and it showed iron line-emission in at least one low-amplitude flare (Corbet et al. 1997).

In recent years A 0538–66 entered a quiescent phase, with outbursts 2–3 orders of magnitude below the early levels and low persistent luminosity (Campana et al. 2002). Using an *XMM-Newton* observation performed in 2002, Kretschmar et al. (2004) found a spectrum well fitted by a featureless power-law model with $\Gamma = 1.9 \pm 0.3$ and estimated a 0.3–10 keV luminosity of $(5\text{--}8) \times 10^{33}$ erg s $^{-1}$. The mechanism presently powering the faint X-ray emission of A 0538–66 is unclear. It could be either a low-rate accretion or the pulsar rotational energy through the shock between the pulsar wind and the inflowing material, as proposed for LSI+61° 303. To our knowledge, no data concerning the radio or GeV–TeV emission of A 0538–66 are available to further investigate the similarities and the possible connection between this source and the “gamma-ray binaries” LSI+61° 303, LS 5039, and PSR B1259–63.

Acknowledgements. Based on observations with the NASA/UK/ASI Swift mission, obtained through the High Energy Astrophysics Science Archive Research Center Online Service, provided by the NASA/Goddard Space Flight Center. We thank the Swift team for making these observations possible, in particular the duty scientists and science planners. The Italian authors acknowledge the support of the Italian Space Agency (contract ASI/INAF I/023/05/0) and the Italian Ministry for University and Research (grant PRIN 2005 02 5417). A.D.L. acknowledges an Italian Space Agency fellowship, M.A.M. a “G. Petrocchi” fellowship of the Osio Sotto (BG) city council. We thank Pat Romano for her help with the Swift/XRT data. We also thank Lara Sidoli, Ada Paizis, Andrea Tiengo, and Stefano Vercellone for useful discussions.

References

- Albert, J., Aliu, E., Anderhub, H., et al. 2006, *Science*, 312, 1771
 Alcock, C., Allsman, R. A., Alves, D. R., et al. 2001, *MNRAS*, 321, 678
 Bignami, G. F., & Hermsen, W. 1983, *ARA&A*, 21, 67
 Bignami, G. F., Caraveo, P. A., Lamb, R. C., Markert, T. H., & Paul, J. A. 1981, *ApJ*, 247, L85
 Bosch-Ramon, V., Paredes, J. M., Ribó, M., et al. 2005, *ApJ*, 628, 388
 Burrows, D. N., Hill, J. E., Nousek, J. A., et al. 2005, *Space Sci. Rev.*, 120, 165
 Campana, S., Stella, L., Israel, G. L., et al. 2002, *ApJ*, 580, 389
 Casares, J., Ribas, I., Paredes, J. M., Martí, J., & Allende Prieto, C. 2005, *MNRAS*, 360, 1105
 Chernyakova, M., Neronov, A., & Walter, R. 2006, *MNRAS*, 372, 1585
 Chevalier, R. A. 2000, *ApJ*, 539, L45
 Corbet, R. H. D., Charles, P. A., Southwell, K. A., & Smale, A. P. 1997, *ApJ*, 476, 833
 Dubus, G. 2006, *A&A*, 456, 801
 Frail, D. A., & Hjellming, R. M. 1991, *AJ*, 101, 2126
 Gehrels, N., Chincarini, G., Giommi, P., et al. 2004, *ApJ*, 611, 1005
 Goldoni, P., & Mereghetti, S. 1995, *A&A*, 299, 751
 Gregory, P. C. 2002, *ApJ*, 575, 427
 Gregory, P. C., & Taylor, A. R. 1978, *Nature*, 272, 704
 Gregory, P. C., Peracaula, M., & Taylor, A. R. 1999, *ApJ*, 520, 376
 Greiner, J., & Rau, A. 2001, *A&A*, 375, 145
 Grundstrom, E. D., Caballero-Nieves, S. M., Gies, D. R., et al. 2007, *ApJ*, 656, 437
 Harrison, F. A., Ray, P. S., Leahy, D. A., Waltman, E. B., & Pooley, G. G. 2000, *ApJ*, 528, 454
 Hartman, R. C., Bertsch, D. L., Bloom, S. D., et al. 1999, *ApJS*, 123, 79
 Hermsen, W., & Kuiper, L. 2007, in *First GLAST Symp.*
 Hermsen, W., Swanenburg, B. N., Bignami, G. F., et al. 1977, *Nature*, 269, 494
 Hutchings, J. B., & Crampton, D. 1981, *PASP*, 93, 486
 Kaspi, V. M., Tavani, M., Nagase, F., et al. 1995, *ApJ*, 453, 424
 Kniffen, D. A., Alberts, W. C. K., Bertsch, D. L., et al. 1997, *ApJ*, 486, 126
 Kretschmar, P., Wilms, J., Staubert, R., Kreykenbohm, I., & Heindl, W. A. 2004, in *ESA Special Publication*, ed. V. Schoenfelder, G. Lichti, & C. Winkler, 552, 329
 Leahy, D. A. 2001, *A&A*, 380, 516
 Leahy, D. A., Harrison, F. A., & Yoshida, A. 1997, *ApJ*, 475, 823
 Martí, J., & Paredes, J. M. 1995, *A&A*, 298, 151
 Mendelson, H., & Mazeh, T. 1989, *MNRAS*, 239, 733
 Mirabel, I. F. 2006, *Science*, 312, 1759
 Paredes, J. M., Marziani, P., Martí, J., et al. 1994, *A&A*, 288, 519
 Paredes, J. M., Martí, J., Peracaula, M., & Ribo, M. 1997, *A&A*, 320, L25
 Paredes, J. M., Martí, J., Ribó, M., & Massi, M. 2000, *Science*, 288, 2340
 Paredes, J. M., Ribó, M., Bosch-Ramon, V., et al. 2007, *ApJ*, 664, L39
 Sidoli, L., Pellizzoni, A., Vercellone, S., et al. 2006, *A&A*, 459, 901
 Skinner, G. K. 1980, *Nature*, 288, 141
 Skinner, G. K., Bedford, D. K., Elsner, R. F., et al. 1982, *Nature*, 297, 568
 Swanenburg, B. N., Bennett, K., Bignami, G. F., et al. 1981, *ApJ*, 243, L69
 Tavani, M., Hermsen, W., van Dijk, R., et al. 1996, *A&AS*, 120, C243
 Taylor, A. R., Young, G., Peracaula, M., Kenny, H. T., & Gregory, P. C. 1996, *A&A*, 305, 817
 White, N. E., & Carpenter, G. F. 1978, *MNRAS*, 183, 11
 White, N. E., Swank, J. H., & Holt, S. S. 1983, *ApJ*, 270, 711
 Zamanov, R. K., Martí, J., Paredes, J. M., et al. 1999, *A&A*, 351, 543